

# Geophysical Research Letters

## RESEARCH LETTER

10.1029/2019GL085902

### Key Points:

- Our experimental analysis reveals striking dune morphodynamic similarity between shallow laboratory flow conditions and deep rivers
- We present the first observation of upper stage plane bed in a shallow laboratory flume that is reached for a Froude number well below unity
- Dune slipface angles show a systematic decrease with increasing entrainment of bed sediment into suspension

### Supporting Information:

- Supporting Information S1

### Correspondence to:

S. Naqshband,  
suleyman.naqshband@wur.nl

### Citation:

Naqshband, S., & Hoitink, A. J. F. (2020). Scale-dependent evanescence of river dunes during discharge extremes. *Geophysical Research Letters*, *47*, e2019GL085902. <https://doi.org/10.1029/2019GL085902>

Received 21 OCT 2019

Accepted 4 FEB 2020

Accepted article online 6 MAR 2020

©2020. The Authors.

This is an open access article under the terms of the Creative Commons Attribution License, which permits use, distribution and reproduction in any medium, provided the original work is properly cited.

## Scale-Dependent Evanescence of River Dunes During Discharge Extremes

S. Naqshband<sup>1</sup>  and A. J. F. Hoitink 

<sup>1</sup>Department of Environmental Sciences, Wageningen University, Wageningen, Netherlands

**Abstract** During high river discharge extremes, the growth of dunes can reach a maximum beyond which a transition to upper stage plane bed may occur, enhancing the river's conveyance capacity and reducing flood risk. Our predictive ability of this bedform regime shift in rivers is exclusively built upon high Froude number flows dominated by asymmetric dunes with steep downstream-facing slipfaces that are rare in natural rivers. By using light-weight polystyrene particles as a substrate in an experimental flume setting, we present striking dune morphodynamic similarity between shallow laboratory flow conditions and deep rivers, preconditioned that both flow and sediment transport parameters are accurately scaled. Our experimental results reveal the first observation of upper stage plane bed in a shallow laboratory flume that is reached for a Froude number well below unity. This work highlights the need to rethink widely used dune scaling relationships, bedform stability diagrams, predictions of flow resistance, and flood risk.

**Plain Language Summary** Dunes are rhythmic shapes at the river bed that significantly increase water levels and the associated flood risk. They can reach heights up to one third of the water depth and often dominate the flow field. Under extremely high river discharges, dunes are observed to undergo a transition phase, after which they are washed out and disappear from the river bed. This morphological transition is expected to substantially reduce water levels and thus flood risk, by enhancing the conveyance capacity of the river during a peak discharge event. Once such circumstances can be predicted with certainty, it will become possible to meet safety standards while reducing the height of the river embankment.

## 1. Introduction

Dunes are periodic sediment structures that arise from the interaction between a flow field and the underlying mobile bed, in fluvial environments dominated by coarse silt, sand, or gravel. The presence of dunes strongly controls sediment transport and flow resistance. They leave a unique signature in sedimentary records, allowing stratigraphic interpretation and reconstruction of current and past climate and landscape evolution, on Earth as well as on other planets (e.g., Ewing et al., 2015; Galeazzi et al., 2018; Runyon et al., 2017).

It is now widely recognized that dunes in large, deep rivers (flow depth > 2.5 m) are unlike dunes formed in flumes and shallow rivers (flow depth < 2.5 m; e.g., Best & Fielding, 2019; Bradley & Venditti, 2017, 2019a, 2019b; Cisneros & Best, 2016; Kostaschuk & Venditti, 2019). Flumes and shallow rivers are dominated by asymmetric, high-angle dunes (HADs), with steep downstream-facing slipfaces at an angle-of-repose of approximately 30° (Figure 1). In contrast, dunes in deep rivers are primarily symmetric, with significantly lower slipface angles, often less than 10° (referred to as low-angle dunes [LADs]). They possess complex leeside morphologies with superimposed bedforms on both the stoss and the lee sides (Galeazzi et al., 2018; Hendershot et al., 2016). Consequently, HADs exhibit a zone of permanent flow separation with high energy losses due to turbulence production (Kwoll et al., 2016; Lefebvre & Winter, 2016), limiting the sediment transport capacity of the flow, whereas LADs are associated with intermittent or absent flow separation, causing significantly less energy losses (Best, 2005; Best & Kostaschuk, 2002; Kwoll et al., 2017; Lefebvre et al., 2016; Motamedi et al., 2012, 2014). In addition to contrasting morphology metrics of dimension and shape, and opposing leeside flow dynamics, HADs and LADs have major kinematic differences in terms of translation and deformation. With increasing flow intensity and transport of bed material into suspension, HADs in flumes decay, make a regime shift, and then wash out to upper stage plane bed (USPB) at a suspension number that is twice lower compared to LADs in deep rivers (Naqshband et al., 2014a; Bradley & Venditti, 2017). This

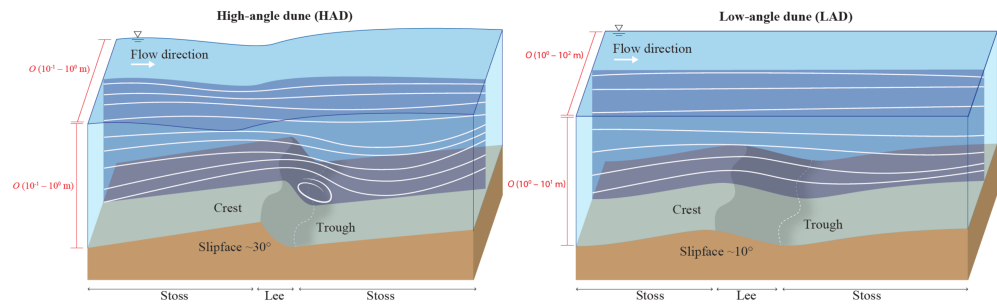


**Figure 1.** Schematic representation of dune morphologies in shallow and deep flow, (a) shallow flow asymmetric high-angle dune (HAD) with steep downstream-facing slipface at the angle-of-repose  $\sim 30^\circ$ , producing a permanent zone of flow separation and showing strong interaction with free water surface due to high Froude number, (b) deep flow symmetric low-angle dune (LAD) with slipface angle  $\sim 10^\circ$ , displaying no interaction with free water surface due to much lower Froude number. The solid white lines in the streamwise-vertical plane highlight the mean flow streamlines along both dune morphologies based on laboratory work by Kwoell et al. (2016).

bedform regime shift during time-varying flows is associated with a significant change in flow resistance and water levels (Nelson et al., 2011).

Although there are several hypotheses about why LADs are generated in deep flows, causative controlling mechanisms are yet poorly understood. Factors widely considered in literature are (i) increased transport of bed material into suspension, (ii) deposition of suspended sediment in dune troughs, and (iii) bedform superimposition and amalgamation (Best & Fielding, 2019). Strong free surface interaction with the bed in shallow laboratory flows on the other hand is considered to be a contributory factor in producing HADs in shallow flows (Andreotti & Claudin, 2013; Fourrière et al., 2010; Naqshband et al., 2014; Unsworth et al., 2018). Recent advances further highlight the potential of maintaining high-angle slipfaces on HADs by granular avalanches, whereas lower slipface angles of LADs have been interpreted as the product of loosely packed liquefied avalanches amplified by downslope currents (Kostaschuk & Venditti, 2019). Whereas sediment transport parameters (e.g., the Shields number and mobility parameter) in deep rivers are usually properly scaled in shallow flume experiments, the Froude number ( $Fr$ )—undoubtedly the second most important bulk flow parameter next to the Reynolds number—is much larger in flumes ( $Fr > 0.32$ ) compared to deep rivers ( $Fr < 0.32$ ; Bradley & Venditti, 2017, 2019a; Fourrière et al., 2010; Holmes & Garcia, 2008; Julien, 1992; Naqshband et al., 2014, 2016, 2017). Although the Froude number is widely accepted to control dune stability and transition to USPB through both linear stability analysis (e.g., Colombini & Stocchino, 2008; Engelund, 1970; Kennedy, 1963; McLean, 1990; Shimizu et al., 2009) and empirical observations (e.g., Naqshband et al., 2017; Nelson et al., 2011; Simons & Richardson, 1966; Southard & Boguchwal, 1990), the physical controlling mechanism that links dune morphology to  $Fr$  remains unexplored to date. The most important reason for this knowledge gap is our inherent limitation of correctly scaling  $Fr$  in the dune stability regime under shallow laboratory flows. Consequently, we are limited in our ability to predict bedform regimes and USPB in rivers by using bedform stability diagrams that are almost entirely based on shallow flow laboratory experiments over HADs (e.g., Kostaschuk & Villard, 1996; Naqshband et al., 2014).

Here we investigate dune morphodynamics in a shallow laboratory flume by using light-weight polystyrene particles as a substrate. Our analysis reveals a striking dune morphodynamic similarity between shallow laboratory flows and deep rivers, preconditioned that both Froude number and sediment transport parameters are well aligned with conditions in deep rivers. We present the first observation of USPB in a shallow laboratory flume that is reached for a Froude number well below unity, paving the way for advancement in our understanding of causative mechanisms governing dune morphology and leeside dynamics.

## 2. Methods and Laboratory Flume Experiments

Experimental conditions were designed to represent natural variability of flow and sediment transport conditions in large, deep rivers. A total of 10 flume experiments were conducted in conditions ranging from regular dunes to USPB, covering a wide range of suspension numbers (bed load dominated [BLD] to mixed load dominated [MLD] and ultimately suspended load dominated [SLD] transport conditions). The Froude

number is kept in the range of what is observed in deep rivers ( $0.17 < Fr < 0.30$ ; see Table S1 in the supporting information). Experiments were conducted in a tilting flume with recirculation facilities for both water and sediment in the Kraijenhoff van de Leur laboratory for Water and Sediment dynamics, Wageningen University and Research (Figure S1). The flume measures  $1.20 \text{ m} \times 0.50 \text{ m} \times 14.4 \text{ m}$  internally (width  $\times$  height  $\times$  length). At the upstream end of the flume, where sediment-rich water reenters, a diffuser is placed to distribute the inflow over the full width of the flume, followed by a stacked pile of PVC tubes that serves as a flow laminator, suppressing turbulence. A fine sediment filter was installed at the downstream end of the flume preventing loss of sediment particles over the flume edge and guaranteeing full recirculation of bed material. A 15-cm-thick layer of uniformly distributed, light-weight polystyrene particles was installed at the flume bed with a density of  $\rho_s = 1,055 \text{ kg/m}^3$ . Polystyrene particles are used in engineering studies as a surrogate for sand in physical scale models where a geometrical scale factor is applied between a model and its prototype natural system, allowing dynamic similarity of both flow and sediment transport parameters (e.g., Hentschel, 2007; Vermeulen et al., 2014). Although polystyrene particles tend to overrepresent the bed sediment mobility, dunes that develop in the polystyrene granulates are similar to the dunes in natural system, especially regarding dune heights (e.g., Vermeulen et al., 2014).

The exact particle-size distribution of polystyrene used in this study was determined with a Microtrac Dry Image Analyzer, giving characteristic particle sizes of  $D_{50} = 2.1 \text{ mm}$  and  $D_{90} = 2.6 \text{ mm}$ . The particle settling velocity distribution was determined by inserting at least 100 particles in still water and tracking individual particle travel times and trajectories over a 0.15-m vertical window (see Figure S2). Flow discharge, initial flow depth, and flume slope were imposed in all experiments, whereas the water surface slope and transport conditions adjusted to these initial conditions by reaching a dynamic equilibrium. Flow discharge was measured continuously with an electromagnetic flow meter. Water levels were also continuously monitored at four points along the centreline of the flume using stilling wells, with each stilling well containing a magnetostrictive linear position sensor. The bed topography was measured during subsequent phases of the experiment (initial dry-bed conditions, initial submerged conditions, and dune dynamic equilibrium) with a line laser scanner where bed elevation is derived from the reflection of light projected on the flume bed using a line laser and a 3-D camera (de Ruijscher et al., 2018). This allows for bed elevation measurements without interacting with the flow. The entire flume bed was scanned with a streamwise resolution of 2 mm and a crosswise resolution of 3 mm, in four parallel partly overlapping swipes, within a period of 2 min. Three evenly distributed transects from the centre of the flume toward both sidewalls were selected to monitor dune morphology (dune height  $\Delta$ , length  $\lambda$ , and slipface angle  $\beta$ ) using a well-established bedform tracking tool (van der Mark et al., 2008). Distributions of  $\Delta$ ,  $\lambda$ , and  $\beta$  were determined over the effective measurement section of the flume (streamwise distance along the flume between 4 and 8 m; see Figure S1). The obtained dune bed statistics are compared with a recently compiled, large data set of HADs and LADs including both laboratory flume experiments and field observations documented in Naqshband et al. (2014) and Bradley and Venditti (2017).

### 3. Results

#### 3.1. Dune Kinematic Evolution to Upper Stage Plane Bed

Measured bed morphology under dynamic equilibrium at BLD (EXP3), MLD (EXP4), and SLD (EXP8 + EXP9) transport conditions illustrates subsequent stages of dune development and transition to USPB (Figure 2). At the BLD transport condition, particles travel through intermittent saltation close to the bed, with horizontal travel distances of 10–100 times the average particle diameter. Events are observed with particles being entrained into suspension from the dune crests, but there is no measureable transport of bed material into suspension. Dune crestlines are clearly 2-D oriented with a relatively low number of superimposed bedforms—a key feature of bedform kinematics—which emerged from dissipation of upstream dunes (Carling et al., 2000; Reesink et al., 2018; Reesink & Bridge, 2009; Venditti et al., 2016). Topographic variability increases at the MLD transport condition with bed sediment readily entrained into suspension. Dunes become higher and longer with deeper scours in the trough (see dune bed characteristics in Table S1). Trains of superimposed bedforms are more abundant on the stoss slopes, causing additional events of dune splitting and merging. Crestlines become 3-D oriented with saddle-shaped sections that form along with spurs, that is, ridges parallel to the mean flow direction, responsible for dune growth and a transition from 2-D to 3-D features (Swanson et al., 2017; Venditti et al., 2016). During the first stage of dune

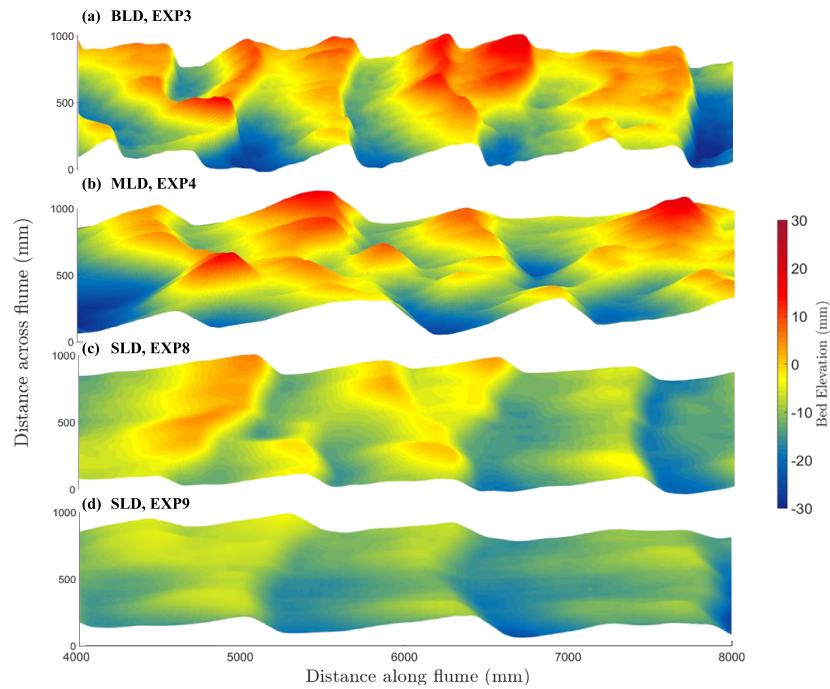


**Figure 2.** Bed morphology under dynamic equilibrium illustrating different stages of dune development and transition to upper stage plane bed, (a) at the bed load dominated (BLD, EXP3), (b) mixed load dominated (MLD, EXP4), and (c and d) suspended load dominated (SLD, EXP8, and EXP9) sediment transport conditions.

transition to USPB at SLD transport conditions (EXP8), flux rates increase substantially compared to the BLD and MLD conditions. Dune lengths further increase, while dune heights decrease due to filling up of the troughs. Superimposed dunes became less persistent, and dune crest orientation strongly altered between 2-D and 3-D. With transport of bed material in full suspension at the final stage of dune transition (EXP9), dune morphology becomes unstable and dune height diminishes due to flattening-out

of dune crests, associated with increasing flow velocity and decreasing flow depth (Naqshband et al., 2014; Reesink et al., 2018). Superimposed dunes vanish throughout the entire flume experiment, implying that they may not play an important role in washing out of host dunes through amalgamation processes, contrary to what is suggested in literature (e.g., Best, 2005; Naqshband et al., 2017).

The spatially averaged relative dune height ( $\Delta/h$ ) in our shallow flow experiments, plotted against Suspension number, illustrates dune kinematic evolution to USPB under low Froude numbers ( $0.17 < Fr < 0.30$ ): dune growth (EXP1 to EXP4), dune stabilization (EXP5 to EXP7), and transition to USPB (EXP8 and EXP9; Figure 3, yellow squares). Unlike any other laboratory flume data in literature aiming to quantify dune growth and transition to USPB (Figure 3, red triangles, with  $0.32 < Fr < 0.84$ ), our shallow flow experimental data with light-weight polystyrene particles show good agreement with dune development and transition as observed in large, deep rivers (Figure 3, blue circles, with  $0.10 < Fr < 0.30$ ). USPB in traditional shallow laboratory flumes is reached for Froude number close to unity (e.g., Guy et al., 1966; Brownlie, 1982, and references therein; Bradley & Venditti, 2017; Naqshband et al., 2016), whereas in rivers, USPB is observed at Froude number range of 0.13 to 0.68 (see Table 2 in Naqshband et al., 2014, for references and additional details). Our experimental results present the first observation of USPB in a shallow laboratory flume that is reached

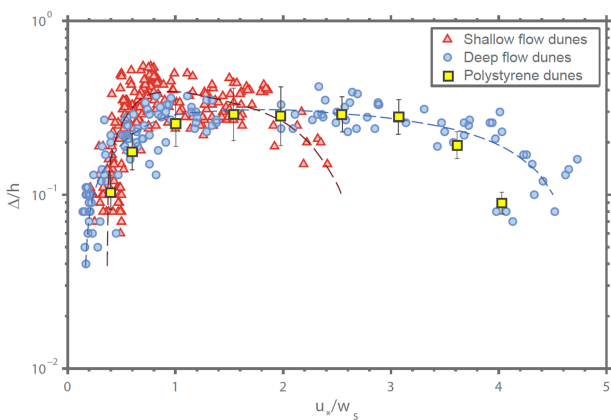


**Figure 3.** Dune growth, stabilization, and transition to upper stage plane bed illustrated by plotting spatially averaged relative dune height ( $\Delta/h$ ) against suspension number ( $u^*/w_s$ ). The yellow squares indicate the shallow flow laboratory experiments with light-weight polystyrene particles ( $0.17 < Fr < 0.30$ ); the error bars show the standard deviations. The red triangles represent the 11 data sets of dune height evolution in shallow flow laboratory experiments with sand ( $0.32 < Fr < 0.84$ ), and the blue circles show the dune height data from seven deep river data sets ( $0.10 < Fr < 0.30$ ), all documented in Naqshband et al. (2014).

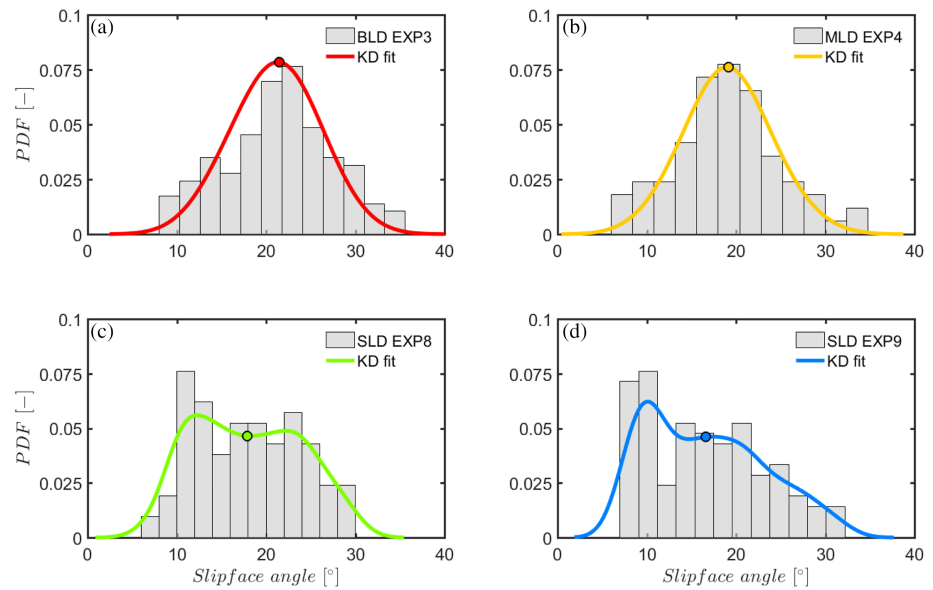


**Figure 4.** Distribution of dune slipface angle for different stages of dune development. The solid lines represent kernel density fits to dune slipface data with circles indicating spatially averaged values, (a) at bed load dominated (BLD, EXP3), (b) mixed load dominated (MLD, EXP4), and (c and d) suspended load dominated (SLD, EXP8, and EXP9) transport conditions.

for Froude number well below unity (EXP10,  $Fr = 0.30$ ; see Table S1). Consequently, these experiments are the first to achieve dynamic similarity between dune transition to USPB observed in flumes and in prototype deep rivers.

### 3.2. Dune Morphology: Dune Shape and Slipface Angle

Dune shape and slipface angle control flow resistance and sediment transport conditions by setting the flow structure behind dunes. Initially, at BLD transport conditions (EXP1 to EXP3), dunes were triangular due to low topographic acceleration and minimal crestral flattening, reflecting bed load avalanching process at dune leesides (Best, 1996; Carling et al., 2000; Unsworth et al., 2018). At slightly higher sediment transport conditions (EXP4), the largest dunes were produced due to deposition at the dune crest promoted by high vertical velocities, and increased trough scour associated with larger Reynold stresses at the flow reattachment point (Table S1). Dunes with long flat crests, often referred to as humpback dunes, linked to increased crestral flattening (Bridge & Best, 1988; Saunderson & Lockett, 1983; Unsworth et al., 2018), appear to dominate the flume bed at higher transport conditions (EXP 5 to EXP9).

In addition to the dune shape that evolves throughout subsequent stages of dune development and transition, the dune leesides adjust to flow conditions and associated changes in sediment transport. Dune slipface angles at BLD and MLD transport conditions closely follow a Gaussian distribution, being symmetric around mean values, and mean values coincide with the corresponding modes (Figures 4a and 4b). With increasing entrainment of bed sediment into suspension at SLD conditions (Figures 4c and 4d), distributions become positively skewed toward lower slipface values, with mean values deviating from the corresponding modes. This observation may be a direct manifestation of a skewed distribution of particle travel distance at SLD transport conditions, whereas a Gaussian, symmetric distribution of particle travel distance is measured at BLD transport condition (Naqshband et al., 2017). Moving from BLD ( $\beta = 22.3^\circ$ , EXP1) to SLD ( $\beta = 16.6^\circ$ , EXP9) transport conditions, spatially averaged slipface angles show a systematic decrease with increasing bed sediment into suspension (Table S1). This reflects the deposition process of suspended sediment in dune troughs; sediment that is picked up from the dune crest not only settles at the dune leeside by avalanching but is increasingly deposited in the dune trough, leading to much lower and gentler leeside angles (e.g., Best & Kostaschuk, 2002; Kostaschuk et al., 2009; Naqshband et al., 2016). The percentage of dunes with slipface angles larger than  $24^\circ$ , and thus possessing fully developed flow separation zones (Lefebvre & Winter, 2016), significantly decreased from 32.1% for EXP1 to 10.3% for EXP9. On the other hand, the percentage of dunes

with slipface angles smaller than  $11^\circ$ —that is, the onset angle for the initiation of flow separation (Lefebvre & Winter, 2016)—increased from 17.6% for EXP1 to 47.0% for EXP9. Most notably, whereas a slipface angle of  $30^\circ$  is the norm for HADs in traditional shallow laboratory flows, these steep slipface angles are an exception for our shallow flow dunes under low Froude number conditions, analogous to observed slipface angles of LADs in deep rivers. Consequently, flow resistance is overestimated in traditional shallow laboratory flows with HADs compared to deep rivers dominated by LADs.

#### 4. Implications for Flow Resistance and Flood Risk

More than a century of research on dunes in laboratory flumes has been conducted under the implicit assumption that high Froude number dunes formed in shallow flows (HADs) can represent dunes in deep rivers (LADs), without considering the changes in processes that may occur (see also Best & Fielding, 2019; Kostaschuk & Venditti, 2019). Consequently, most of our understanding and extensively applied quantitative formulations of dune dimensions, kinematics, dynamics, flow resistance, and sediment transport originate from experimental investigations of fixed and mobile HADs in shallow laboratory flumes. This has resulted in major discrepancies between field observations and predictions of sediment transport rates, channel migration and dynamics, and interpretation of dune deposits and their use in palaeohydraulic reconstructions (e.g., Bathurst, 2007; Best & Fielding, 2019; Hergault et al., 2010; Reesink & Bridge, 2009; Wilcock, 2001). Ma et al. (2017), for instance, showed that the widely used Engelund-Hansen sediment transport equation underpredicts sediment transport rates in Huanghe river by an order of magnitude. They attribute this to observations of low-amplitude, long-crested dunes at the Huanghe riverbed, without flow separation zones at their leesides, and thus, generating negligible form roughness. While developing the Engelund-Hansen formula, four shallow flow data sets of Guy et al. (1966) were used with HADs covering the flume bed (Engelund & Hansen, 1967). These HADs with angle-of-repose slipfaces possess permanent flow separation zones that generate a significant amount of turbulence behind their crests, and hence, increase flow resistance by form roughness, and reduce sediment transport capacity of the flow (e.g., Kwoil et al., 2017; Lefebvre et al., 2016; Ma et al., 2017). Our analysis reveals the dominance of LADs in shallow laboratory flow preconditioned that the Froude number is accurately scaled, here achieved with the use of polystyrene granulates. Our results demonstrate that 18.6% of all dunes in the dune stability regime possess slipface angles larger than  $24^\circ$  and thus have fully developed flow separation zones. Flow separation does not occur for 30.9% of all dunes with slipface angles smaller than  $11^\circ$ . Hence, the methodology presented here will allow to improve the established formulations of dune dimensions and flow resistance that are commonly derived from HAD flume experiments. Although both Froude number and sediment transport parameter are properly scaled in shallow flume experiments using polystyrene granulates, Reynolds number may be 1 or 2 orders of magnitude larger in rivers. It is not yet clear to what extent this mismatch in Reynolds scale factor may impact dune morphodynamics, and therefore, care must be taken while improving established dune height and length predictors.

Bradley and Venditti (2017) reevaluated dune height scaling relations by compiling an impressive data set with 664 reach-averaged height observations from both flume and field studies. They proposed a simple depth-scaling relation with added statistical uncertainty for the prediction of dune height from flow depth but also concluded that flow depth may not be the fundamental control on dune morphology and that the apparent scaling of dune height with flow depth may be indirect, emerging from bed shear stress and shear velocity. The proposed flow depth-scaling relation is a useful tool for engineering, geomorphological, or sedimentological problems, as it gives both a forward prediction of dune height from flow depth, and an inverse prediction of flow depth from dune height. However, a universal tool to study sediment structures formed by ancient dunes on Earth and on other planetary surfaces such as Mars, Saturn, Venus, and Titan requires a dimensionless parameterization of flow dynamics and sediment characteristics to account for variation in gravity, sediment density, and fluid viscosity (e.g., Ewing et al., 2015; Jackson et al., 2015; Lü et al., 2017). Our experimental work with lightweight polystyrene particles allows to achieve higher dynamic similarity, yielding an improved physical model setting under highly controlled conditions that will facilitate the prediction and interpretation of fluvial dunes across scales.

It is widely recognized that due to global warming and the associated climate change, intense rainfall will bring extreme peak discharges that will have major consequences for riverbed morphology and water

levels along the course of many rivers worldwide. Recent climate studies show that flood peaks with return periods above 100 years are projected to double in frequency of occurrence within three decades, substantially increasing flood risk (e.g., Alfieri et al., 2015). Under these extreme high discharges, however, dunes may undergo a transitional regime after which they wash out to USPB (Naqshband, 2014, Nabi et al., 2015, Hulscher et al., 2017). This morphological transition of dunes will reduce flow resistance, and thus, decrease water levels and flood risk, leading to a self-regulation process in rivers. Currently, lacking knowledge of dune morphodynamics under extreme discharges obstructs our capability to predict the occurrence of this morphological transition in rivers, and its contribution to reducing flood risk. Dune morphodynamics including the evolution to USPB presented in this study shows a striking similarity with observations in large rivers, paving the way for advancement in our understanding of causative mechanisms governing dune morphodynamics and bedform regime shifts under extreme discharges.

#### Acknowledgments

Partial funding for this research was provided by the Department of Environmental Sciences at Wageningen University and the Dutch Ministry of Infrastructure and Environment (Rijkswaterstaat, Fund 5160957319). We thank Jeff Nittrouer and an anonymous reviewer for their helpful comments and suggestions. The data used in this manuscript are archived and made publicly available through the 4TU.Centre for Research Data (Naqshband, S., 2019, Supporting Information for "Scale-dependent evanescence of river dunes during discharge extremes." 4TU.Centre for Research Data. Data Set. <https://doi.org/10.4121/uuid:63d58eae-ecd1-4065-a8d3-297fce0aa022>).

#### References

- Alfieri, L., Burek, P., Feyen, L., & Forzieri, G. (2015). Global warming increases the frequency of river floods in Europe. *Hydrology and Earth System Sciences*, *19*, 2247–2260.
- Andreotti, B., & Claudin, P. (2013). Aeolian and subaqueous bedforms in shear flows. *Philosophical Transactions of the Royal Society A*, *371*, 20120364.
- Bathurst, J. C. (2007). Effect of coarse surface layer on bed-load transport. *Journal of Hydraulic Engineering*, *133*, 1192–1205.
- Best, J. L. (1996). The fluid dynamics of small-scale alluvial bedforms. In P. A. Carling & M. R. Dawson (Eds.), *Advances in fluvial dynamics and stratigraphy* (pp. 67–125). Chichester: John Wiley and Sons.
- Best, J. L. (2005). The fluid dynamics of river dunes: A review and some future research directions. *Journal of Geophysical Research*, *110*, F04S02. <https://doi.org/10.1029/2004JF000218>
- Best, J. L., & Fielding, C. R. (2019). Describing fluvial systems: Linking processes to deposits and stratigraphy. *Geological Society of London, Special Publication*, *488*, 152–166.
- Best, J. L., & Kostaschuk, R. (2002). An experimental study of turbulent flow over a low-angle dune. *Journal of Geophysical Research*, *107*(C9), 3135. <https://doi.org/10.1029/2000JC000294>
- Bradley, R. W., & Venditti, J. G. (2017). Re-evaluating dune scaling relations. *Earth-Science Reviews*, *165*, 356–376.
- Bradley, R. W., & Venditti, J. G. (2019a). Transport scaling of dune dimensions in shallow flows. *Journal of Geophysical Research: Earth Surface*, *124*, 526–547. <https://doi.org/10.1029/2018JF004832>
- Bradley, R. W., & Venditti, J. G. (2019b). The growth of dunes in rivers. *Journal of Geophysical Research: Earth Surface*, *124*, 548–566. <https://doi.org/10.1029/2018JF004835>
- Bridge, J. S., & Best, J. L. (1988). Flow, sediment transport and bedform dynamics over the transition from dunes to upper-stage plane beds: Implications for the formation of planar laminae. *Sedimentology*, *35*, 753–763.
- Brownlie, W. (1982). Prediction of flow depth and sediment transport in open channels. *Ph.D. dissertation, California Institute of Technology*, Pasadena, CA, 22–33.
- Carling, P. A., Golz, E., Orr, H. G., & Radecki-Pawlik, A. (2000). The morphodynamics of fluvial sand dunes in the River Rhine, near Mainz, Germany. I. Sedimentology and morphology. *Sedimentology*, *47*, 227–252.
- Cisneros, J., & Best, J. (2016). Low-angle dunes in big rivers: Morphology, occurrence and speculations on their origin. In *Marine and River Dune Dynamics – MARID V*, North Wales, UK, 4–5 April.
- Colombini, M., & Stocchino, A. (2008). Finite-amplitude river dunes. *Journal of Fluid Mechanics*, *611*, 283–306.
- de Ruijsscher, T. V., Hoitink, A. J. F., Dinnissen, S., Vermeulen, B., & Hazenberg, P. (2018). Application of a line laser scanner for bed form tracking in a laboratory flume. *Water Resources Research*, *54*, 2078–2094. <https://doi.org/10.1002/2017WR021646>
- Engelund, F. (1970). Instability of erodible beds. *Journal of Fluid Mechanics*, *42*, 225–244.
- Engelund, F., & Hansen, E. (1967). *A monograph on sediment transport in alluvial streams*. Copenhagen: Teknisk Forlag.
- Ewing, R. C., Hayes, A. G., & Lucas, A. (2015). Sand dune patterns on Titan controlled by long-term climate cycles. *Nature Geoscience*, *8*, 15–19.
- Fourrière, A., Claudin, P., & Andreotti, B. (2010). Bedforms in a turbulent stream: Formation of ripples by primary linear instability and of dunes by nonlinear pattern coarsening. *Journal of Fluid Mechanics*, *649*, 287–328.
- Galeazzi, C. P., Almeida, R. P., Mazoca, C. E. M., Best, J. L., Freitas, B. T., Ianniruberto, M., et al. (2018). The significance of superimposed dunes in the Amazon River: Implications for how large rivers are identified in the rock record. *Sedimentology*, *65*, 2388–2403.
- Guy, H. P., Simons, D. B., & Richardson, E. V. (1966). *Summary of alluvial channel data from flume experiments, 1956–61*. Geological Survey Professional Paper 462-I (Vol. 96). Washington: United States Government Publishing Office.
- Hendershot, M. L., Venditti, J. G., Bradley, R. W., Kostaschuk, R. A., Church, M., & Allison, M. A. (2016). Response of low-angle dunes to variable flow. *Sedimentology*, *63*, 743–760.
- Hentschel, B. (2007). *Hydraulische Flussmodelle mit beweglicher Sohle; Mitteilungen 90*. Karlsruhe, Germany: Bundesanstalt für Wasserbau.
- Hergault, V., Frey, P., Métivier, F., Barat, C., Ducottet, C., Bohm, T., & Ancey, C. (2010). Image processing for the study of bedload transport of two-size spherical particles in a supercritical flow. *Experiments in Fluids*, *49*, 1095–1107.
- Holmes, R. R. Jr., & Garcia, M. H. (2008). Flow over bedforms in a large sand-bed river: A field investigation. *Journal of Hydraulic Research*, *46*, 322–333.
- Hulscher, S. J. M. H., Daggenvoorde, R. J., Warmink, J. J., Vermeer, K., & van Duin, O. (2017). River dune dynamics in regulated rivers. 1–4. *Abstract from 4th International Symposium on Shallow Flows, ISSF 2017*, Eindhoven, Netherlands.
- Jackson, D. W. T., Bourke, M. C., & Smyth, T. A. G. (2015). The dune effect on sand-transporting winds on Mars. *Nature Communications*, *6*, 8796.
- Julien, P. Y. (1992). Study of bedform geometry in large rivers. *Rep. Q1389*, Delft Hydraulics, Emmeloord, Netherlands.
- Kennedy, J. F. (1963). The mechanics of dunes and anti-dunes in erodible bed channels. *Journal of Fluid Mechanics*, *16*, 521–544.
- Kostaschuk, R., Shugar, D., Best, J. L., Parsons, D., Lane, S., Hardy, R., & Orfeo, O. (2009). Suspended sediment transport and deposition over a dune: Río Paraná, Argentina. *Earth Surface Processes and Landforms*, *34*, 1605–1611.

- Kostaschuk, R. A., & Venditti, J. G. (2019). Why do large, deep rivers have low-angle dune beds? *Geology*. <https://doi.org/10.1130/G46460.1>
- Kostaschuk, R. A., & Villard, P. V. (1996). Flow and sediment transport over large subaqueous dunes: Fraser River, Canada. *Sedimentology*, *43*, 849–863.
- Kwoll, E., Venditti, J. G., Bradley, R. W., & Winter, C. (2016). Flow structure and resistance over subaqueous high-and low-angle dunes. *Journal of Geophysical Research: Earth Surface*, *121*, 545–564. <https://doi.org/10.1002/2015JF003637>
- Kwoll, E., Venditti, J. G., Bradley, R. W., & Winter, C. (2017). Observations of coherent flow structures over subaqueous high- and low-angle dunes. *Journal of Geophysical Research: Earth Surface*, *5*, 2244–2268. <https://doi.org/10.1002/2017JF004356>
- Lefebvre, A., Paarlberg, A. J., & Winter, C. (2016). Characterising natural bedform morphology and its influence on flow. *Geo-Marine Letters*, *36*, 379–393.
- Lefebvre, A., & Winter, C. (2016). Predicting bed form roughness: The influence of lee side angle. *Geo-Marine Letters*, *36*, 121–133.
- Lü, P., Narteau, C., Dong, Z., Rozier, O., & Courrech du Pont, S. (2017). Unravelling raked linear dunes to explain the coexistence of bedforms in complex dune fields. *Nature Communications*, *8*, 14,239.
- Ma, H., Nittrouer, J. A., Naito, K., Fu, X., Zhang, Y., Moodie, A. J., et al. (2017). The exceptional sediment load of fine-grained dispersal systems: Example of the Yellow River, China. *Science Advances*, *3*(5), e1603114. <https://doi.org/10.1126/sciadv.1603114>
- McLean, S. R. (1990). The stability of ripples and dunes. *Earth Science Reviews*, *29*, 131–144.
- Motamedi, A., Afzalimehr, H., Gallichand, J., & Abadi, E. F. N. (2012). Lee angle effects in near bed turbulence: An experimental study on low and sharp angle dunes. *International Journal of Hydraulic Engineering*, *1*, 68–74.
- Motamedi, A., Afzalimehr, H., Zenz, G., & Galoie, M. (2014). RANS simulations of flow over dunes with low lee and sharp lee angles. In P. Gourbesville, J. Cunge, & G. Caignaert (Eds.), *Advances in Hydroinformatics, Springer Hydrogeology* (pp. 525–533). Singapore: Springer.
- Nabi, M., Kimura, I., Hsu, S. M., Giri, S., & Shimizu, Y. (2015). Computational modeling of dissipation and regeneration of fluvial sand dunes under variable discharges. *Journal of Geophysical Research: Earth Surface*, *120*, 1390–1403. <https://doi.org/10.1002/2014JF003364>
- Naqshband, S. (2014). Morphodynamics of river dunes: Suspended sediment transport along mobile dunes and dune development towards upper stage plane bed (PhD thesis). Enschede: University of Twente.
- Naqshband, S., McElroy, B., & Mahon, R. C. (2017). Validating a universal model of particle transport lengths with laboratory measurements of suspended grain motions. *Water Resources Research*, *53*, 4106–4123. <https://doi.org/10.1002/2016WR020024>
- Naqshband, S., Ribberink, J. S., & Hulscher, S. J. (2014). Using both free surface effect and sediment transport mode parameters in defining the morphology of river dunes and their evolution to upper stage plane beds. *Journal of Hydraulic Engineering*, *140*, 06014010.
- Naqshband, S., van Duin, O. J. M., Ribberink, J. S., & Hulscher, S. J. M. H. (2016). Modelling river dune development and dune transition to upper stage plane bed. *Earth Surface Processes and Landforms*, *41*, 323–335.
- Nelson, J. M., Burman, A. R., Shimizu, Y., McLean, S. R., Shreve, R. L., & Schmeeckle, M. (2011). Bedform response to flow variability. *Earth Surface Processes and Landforms*, *36*, 1938–1947.
- Reesink, A. J., Parsons, D., Ashworth, P., Best, J., Hardy, R., Murphy, B., et al. (2018). The adaptation of dunes to changes in river flow. *Earth-Science Reviews*, *185*, 1065–1087.
- Reesink, A. J. H., & Bridge, J. S. (2009). Influence of superimposed bedforms and flow unsteadiness on the formation of cross strata in dunes and unit bars—Part 2. Further experiments. *Sedimentary Geology*, *222*, 274–300.
- Runyon, K. D., Bridges, N. T., Ayoub, F., Newman, C. E., & Quade, J. J. (2017). An integrated model for dune morphology and sand fluxes on Mars. *Earth and Planetary Science Letters*, *457*, 204–212.
- Saunderson, H. C., & Lockett, F. P. (1983). Flume experiments on bedforms and structures at the dune-bed transition. In J. Collinson & J. Lewin (Eds.), *Mod Anc Fluvial Syst* (pp. 49–58). Waterloo: Wilfrid Laurier University.
- Shimizu, Y., Giri, S., Yamaguchi, I., & Nelson, J. (2009). Numerical simulation of dune-flat bed transition and stage-discharge relationship with hysteresis effect. *Water Resources Research*, *45*, W04429. <https://doi.org/10.1029/2008WR006830>
- Simons, D. B., & Richardson, E. V. (1966). Resistance to flow in alluvial channels. *Geological Survey Professional Paper*, *24* (422-J), U.S. Dept. of the Interior, Washington, DC, 24.
- Southard, J. B., & Boguchwal, L. (1990). A. Bed configuration in steady unidirectional water flows: Part 2. Synthesis of flume data. *Journal of Sedimentary Research*, *60*, 658–679.
- Swanson, T., Mohrig, D., Kocurek, G., Perillo, M., & Venditti, J. (2017). Bedform spurs: A result of a trailing helical vortex wake. *Sedimentology*, *65*, 191–208.
- Unsworth, C. A., Parsons, D. R., Hardy, R. J., Reesink, A. J. H., Best, J. L., Ashworth, P. J., & Keevil, G. M. (2018). The impact of none-equilibrium flow on the structure of turbulence over river dunes. *Water Resources Research*, *54*, 6566–6584. <https://doi.org/10.1029/2017WR021377>
- Van der Mark, C. F., Blom, A., & Hulscher, S. J. (2008). Quantification of variability in bedform geometry. *Journal of Geophysical Research*, *113*, F03020. <https://doi.org/10.1029/2007JF000940>
- Venditti, J. G., Lin, C.-Y. M., & Kazemi, M. (2016). Variability in bedform morphology and kinematics with transport stage. *Sedimentology*, *63*, 1017–1040.
- Vermeulen, B., Boersema, M. P., Hoitink, A. J. F., Sieben, J., Sloff, C. J., & van der Wal, M. (2014). River scale model of a training dam using lightweight granulates. *Journal of Hydrological Research*, *8*, 88–94.
- Wilcock, P. R. (2001). Toward a practical method for estimating sediment-transport rates in gravel bed-rivers. *Earth Surface Processes and Landforms*, *26*, 1395–1408.